Journal of Structural Geology, Vol. 12, No. 3, pp. 365 to 373, 1990
Printed in Great Britain

0191-8141/90 $03.00+0.00

Experimental mullions at single and double interfaces

DIMITRIOS SOKOUTIS

The Hans Ramberg Tectonic Laboratory, Department of Mineralogy and Petrology, Institute of Geology, Uppsala University, Box 555, S-751 22 Uppsala, Sweden

(*Received* 11 *March* 1988; *accepted in revised form* 30 *October* 1989)

Abstract—The development of mullions at single and double interfaces bounding single layers has been modelled by shortening interfaces or layers with initial irregularities at nearly constant strain rates. The experiments involved a low bulk viscosity ratio, $m = 1/2$ in strain-rate softening materials, in which a mixture of barium sulphate + silicone putty (viscosity, $\eta_L = 2.5 \times 10^6$ Pa s and power law exponent $n \simeq 3$) represented the incompetent material of the layer, and a Plastilina + silicone putty mixture ($\eta_H = 5.5 \times 10^6$ Pa s and $n \simeq 7.1$) represented the more competent host material.

The key feature of this experimental work was the study of the growth rates of initially nearly sinusoidal perturbations at finite strains. Initial irregularities in the single interface amplified unexpectedly fast at constant rates until ~15% bulk shortening (BS), but showed no tendency to develop a dominant wavelength.

Only one of the contacts of the incompetent single layers was given initial sinusoidal irregularities. This geometric form was chosen in order to see whether the planar interface favoured the development of symmetric or antisymmetric mullions. The two initially asymmetric interfaces failed to interact and showed no tendency to develop a dominant wavelength. However, a tendency towards antisymmetric fold mullions appeared at ~20% bulk shortening and further shortening (~40% BS) led to the same mullion products (i.e. 'flames', etc.) already described by the author in incompetent single layers with much larger viscosity contrasts. The final geometry of mullions from ~40% BS and above, appeared to be independent of viscosity contrast. Mullions amplified dynamically only up to ~30% shortening and then the soft material started to move back into the main body of the incompetent layer as the mullions 'closed up'.

INTRODUCTION

THE structures that develop in progressively strained originally planar contacts between rocks of different rheological properties are known as lobes and cusps in axial profile (Fig. 1d). Rounded lobes are convex into the less competent material, and they alternate with sharp cusps which point into the more competent material. Lobe and cusp structures in three dimensions are commonly cylindrical and known as mullions, an architectural term based on an old French adjective meaning 'medial' (Bates & Jackson 1980).

Many structural geologists probably follow Smith's (1975) genetic definition and assume that mullions imply shortening along the interface between rocks of different competence. As similar structures can be created by other mechanisms (e.g. load casts, Ramsay 1967, fig. 7.47, Cobbold 1969a) the term fold mullions (Wilson 1953, 1961) should perhaps be used for the mullions in shortened interfaces. The latter are the kind considered here.

Previous theoretical studies (Biot 1965, Ramberg 1970, 1981, Smith 1975, Fletcher 1982), numerical calculations (Dieterich & Onat 1969) and experiments (Ramsay 1967, Cobbold 1969a) have concentrated on a single deformed interface, and all but Smith (1977) assumed Newtonian fluid behaviour. Smith (1975) first introduced a general linear hydrodynamic stability theory to describe the onset of folding, boudinage and inverse folding, as well as mullions, in single Newtonian layers in a semi-infinite host. Smith's theoretical results suggest that all the abovementioned structures are due to the same mechanism, 'a secondary flow (associated with the perturbation of the interface(s)) driven by an interfacial discontinuity in normal stress', during shortening parallel or perpendicular to competent or incompetent single layers (Smith 1975). According to Smith (1975) the dominant wavelength of all these structures depends on the layer thickness and the ratio, $m = \mu_L/\mu_H$ of viscosity of the layer (μ_L) to that of the host (μ_H). Mullions form when compression acts parallel to a layer with a viscosity lower than that of its host.

Smith (1977) admitted that the theoretical results of his Newtonian model appeared to severely underestimate the growth rates for mullions. The total normalized growth rate used here is based on Smith (1977): total normalized growth rate γ_T = normalized amplitude divided by natural strain parallel to the layer. In 1977, Smith generalized his 1975 Newtonian theory so as to include non-Newtonian behaviour, because it is becoming increasingly apparent that rock deformation is likely to involve non-Newtonian rheological behaviour (see, for example, fig. 3 in Weijermars & Schmeling 1986). The introduction of non-Newtonian flow both increases the growth rates and alters the dominant wavelengths of each of the abovementioned instabilities. The general theory accounts for the short wavelength folds common in rocks and suggests that mullions and boudins are only likely in strain-rate softening hosts (Smith 1977, 1979).

Smith's (1975, 1977) theory raises two very important questions with regard to mullions. First, the theory (Smith 1975, fig. 11; see also Fletcher 1982) predicts all mullions, even those with finite amplitudes, to be symmetrical and have pinch-and-swell-like geometries (Fig.

1a). In contrast, field data (Cobbold 1969b, 1976, Talbot 1983, Sokoutis 1987) and experiments (Sokoutis 1987) suggest that mullions tend to acquire antisymmetric (fold-like) geometries (Fig. 1b). Why is there this discrepancy? Second, does the dominant wavelength predicted by infinitesimal theory apply to finite strains? Experimental mullions in Newtonian fluids with high (>1/20) viscosity contrasts displayed no tendency towards a dominant wavelength at finite strains (Sokoutis 1987).

This work reports an experimental investigation into the tendency of single and paired active interfaces to develop mullions with a dominant wavelength, λ_d, in non-Newtonian fluids with an effective viscosity contrast of less than 1/10. Such low viscosity ratios were prompted by Pfiffner & Ramsay's (1982) suggestions that $m < 1/10$ is common in geological deformations. Another aim was to explore the discrepancies between the predictions of Smith's infinitesimal theory and earlier experiments on mullions.

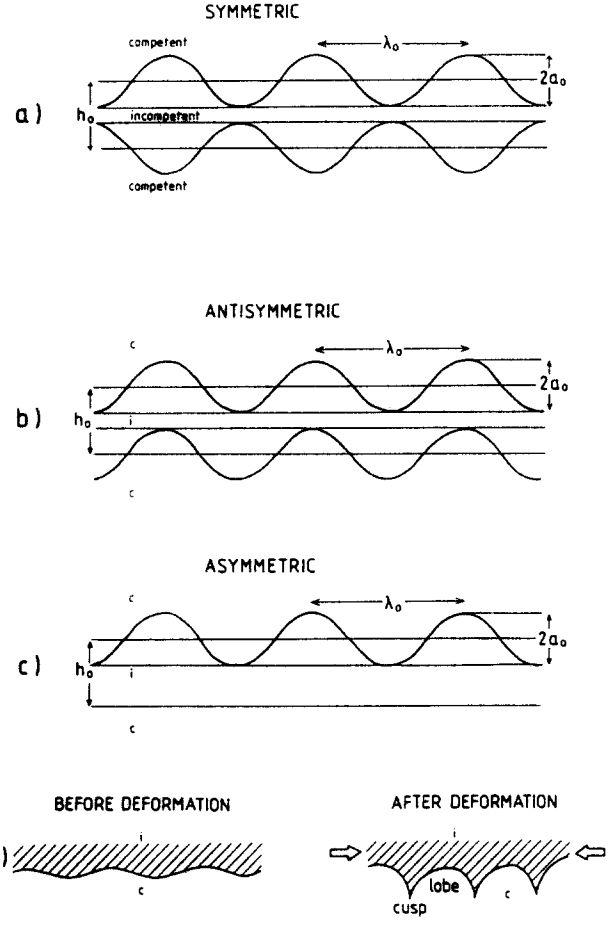

Fig. 1. Classification of structures in incompetent layers based on initially sinusoidal interfaces: (a) symmetric, (b) antisymmetric, (c) asymmetric (where λ_o is the initial wavelength, a_o is the initial amplitude and h_o is the initial thickness). (d) Deviation of an early sinusoidal shape (L. H. S.) leading to the development of fold mullions (R. H. S.) in a single interface due to contact shortening, modelled here.

METHODS

Materials

To study the development of mullions at low ratios of effective viscosity but with strongly non-Newtonian behaviour, two types of material were used: (1) Mixture A is an homogeneous mixture of 67 wt% Plastilina (50% red and 50% white) and 33 wt % 'Rhodorsil Gomme GSIR', a silicone bouncing putty; and (2) Mixture B is an homogeneous mixture of 68 wt % powdered barium sulphate ($BaSO_4$) and 32 wt % 'Rhodorsil Gomme GSIR'. A was used as the host material, B was used as the incompetent layer. Minor amounts of iron oxide pigment were used to impart a colour contrast between layer and host.

Plastilina is the Swedish version of Harbutt's Plasticine (McClay 1976) and contains quartz, kaolinite, hydrated hallosite, K-feldspar and microcline (Weijermars 1986). The volume of the liquid phase in Plastilina is extremely small compared with the amount in bouncing putties, and their different colours are due to liquid pigments (Weijermars 1986). The silicone bouncing putty 'Rhodorsil Gomme CSIR', with Newtonian rheology, is supplied by Rhône-Poulenc of Paris. It becomes non-Newtonian after mixing with either Plastilina or barium sulphate as the concentration of solid particles is increased (Onogi & Matsumoto 1981). The rheological properties in the mixtures were determined by using a HAAKE steady-state extrusion viscometer as well as a cylindrical viscometer (Weijermars 1986).

The general equation for power-law creep is assumed to be:

$$\dot{\gamma} = C_1\sigma^{n_1} + C_2\sigma^{n_2} + \ldots + C_N\sigma^{n_N}, \qquad (1)$$

where $n_N \geq 1$ is the power-law exponent, $\dot{\gamma}$ the shear-strain rate (or engineering strain rate), σ the shear stress, and C_N a constant which depends on P,T conditions and other factors. By assuming flow to be dominated by a single mechanism, equation (1) takes the simpler form:

$$\dot{\gamma} = C\sigma^N. \qquad (2)$$

Figure 2 shows the properties of the two materials used here and some others. The power-law exponent, n, is equal to the inverse of the slope on the graph. A slope of 1/1 on Fig. 2 implies $n = 1$, and lower slopes mean $n > 1$.

Strain rates in the range of 3.6×10^{-4}–6.8×10^{-4} s^{-1} for the experiments reported here are calculated using changes in natural strain rate ($\dot{\varepsilon}$). To be able to use Fig. 2 we have to relate $\dot{\gamma}$, the engineering shear-strain rate, and the normal natural-strain rate $\dot{\varepsilon}$, using the relationship

$$\dot{\gamma} = 2\dot{\varepsilon}. \qquad (3)$$

The effective viscosity can be expressed as:

$$\eta = \frac{\sigma}{\dot{\gamma}}. \qquad (4)$$

For Mixture A the effective viscosity ranged between 5.5 $\times 10^6$ and 2.9 $\times 10^6$ Pa s with $n \simeq 7.1$ (Fig. 2). For

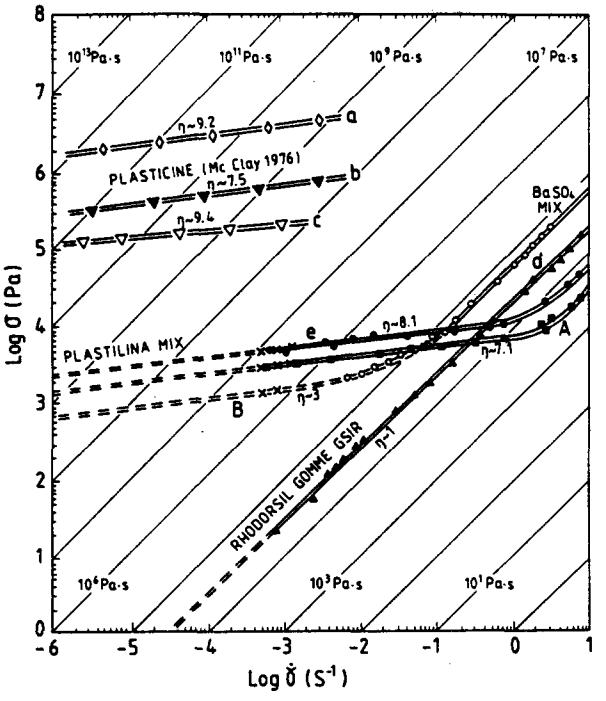

Fig. 2. Flow curves (a–e and A, B) for Plastilina-like materials and Rhodorsil Gomme–$BaSO_4$ mixture material, where $\dot{\gamma}$ represents the engineering strain rate. Materials a–c: standard hard, standard white and especially soft Plasticine, respectively, of Harbutt's Plasticine Ltd, (U.K.) at 25°C (from McClay 1976, fig. 2); Material d: Bouncing Putty (Rhodorsil Gomme GSIR) of the Société des Usines Chimiques Rhônes-Poulenc (France); Material e: mixture of red and white Plastilina (50% of each) and Rhodorsil Gomme of wt % 75:25, respectively; Material A: mixture of red and white Plastilina (50% of each) and Rhodorsil Gomme of wt % 67:33, respectively—competent fluid in this work; Material B: mixture of barium sulphate ($BaSO_4$) and Rhodorsil Gomme of wt % 68:32, respectively—incompetent fluid in this work. Materials d, e and A, B were at steady-state flow of strains larger than 10%, measured by both rotor-viscometer and HAAKE extrusion viscometer at 24°C.

Mixture B the effective viscosity ranged between 2.5×10^6 and 1.5×10^6 Pa s with $n \simeq 3.0$ (Fig. 2). The bulk viscosity ratio, m, ranged from 1/2.2 (at ~3% BS) to m = 1/1.93 (at ~50% BS). This is because the plates of the pure-shear box move with constant velocity and not at constant strain rate. For the variation in strain rates, see Sokoutis (1987, fig. 5). The experimental measurements of growth rate were confined to bulk shortening of <~20%. A constant m of 1/2.2 can be assumed up to this limit, although this does not take into account local viscosity changes due to changes in the shape of the incompetent layer. All viscosity measurements and model deformation took place at 24°C ± 2°C.

Model construction

The experimental approach for finding the dominant wavelength of mullions, λ_d, was based on the study of the growth rates of initial perturbations of nearly sinusoidal shape and 0.025 cm amplitude. The dominant wavelength is expected to develop from the perturbation with the highest growth rate. By having one interface sinusoidal and the other planar, it was possible to see whether the planar interface tended to develop symmetric or antisymmetric mullions. Another advantage of such an asymmetric initial shape (Chadwick 1976) (Fig. 1c) is that by having such simple initial conditions of wavelength, amplitude and thickness, it is easy to monitor any changes during deformation.

For each experiment, a block of Plastilina–silicone putty mixture representing the competent host was centrifuged for 20 min at 1000 g to remove air bubbles. This block was then halved (to 'A' and 'C' in Fig. 3a) and the initial sinusoidal surface was pressed onto one face of one block using a wooden mould. Both blocks were then cut into a rectangular 7 × 8 × 8 cm parallelepiped. The incompetent single layer ('B' in Fig. 3b) was prepared in a similar way as block 'A' with different thicknesses for each experiment. The three components were pushed smoothly together by perspex plates with the incompetent layer embedded in the middle (Fig. 3c). A similar procedure with the same model materials was used for constructing the single interface.

Model deformation

The assemblage block was shortened along the length of the incompetent layer in the squeeze box described in Sokoutis (1987) after the outer surfaces had been lubricated by light machine oil. After compression to different degrees of bulk shortening, the models were carefully removed, sliced perpendicular to the mullion axes, and the amplitudes of the structures were measured as described in Sokoutis (1987).

Limitations of the method

The accuracy of the results may be influenced by slight inhomogeneities in the mixtures or by a departure from ideal sinusoidal shape of the initial disturbances. Disturbances may also have been introduced during the slicing of the model and slight inaccuracies are also likely during measurement of amplitude. Effects due to volume changes during the experiments have not been quantified but are considered negligible. All such inaccuracies are considered minor and unlikely to influence the main conclusions.

RESULTS

Smith (1977) defined the normalized growth rate as $(da/a)/(dL/L)$. After integration the total normalized growth rate $\gamma_T = \ln(a/a_o)/\ln(L/L_o)$. In order to determine γ_T, $\ln(a/a_o)$ (normalized amplitude) is plotted vs $\ln(L/L_o)$ (natural strain parallel to the layer), where a_o, a, are the initial and final disturbance amplitudes, and L_o, L, are the initial and final lengths of a passive line element far from but parallel to the layer (Fig. 6). The slope of the curve at any point equals the growth rate (Neurath & Smith 1982). Table 1 summarizes the initial conditions of all the experiments, and Fig. 4 shows both the normalized total growth rate, γ_T, and dynamic growth rate, γ_d, of the experimental mullions as a function of the normalized wavelength.

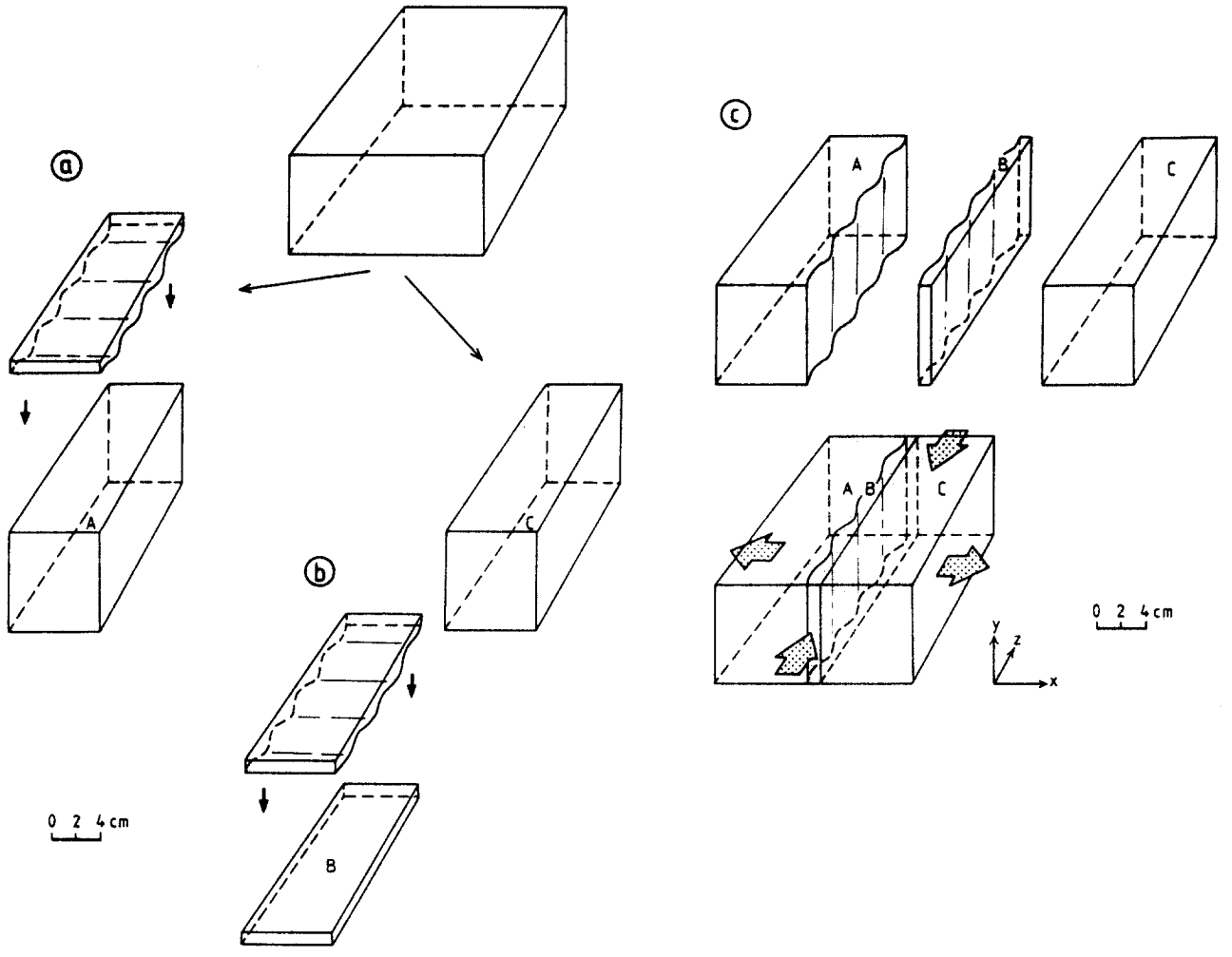

Fig. 3. (a–c) The model parts before and after assembly. Compression was horizontal along the vertical incompetent layer. Vertical movement was prevented by rigid perspex plates on the top and bottom of the pure shear box (Sokoutis, 1987). Lateral expansion/thickening was kept planar using contracting plates kept in place by air-filled bladders.

The normalized wavelength, λ_o/h_o (where λ_o = initial wavelength and h_o = initial thickness of the incompetent layer) of the initial experimental mullions, ranged from ~2.2 to 40. Since the measurements on growth rates were based on the progressive deformation of models with an initial wavelength, dots on the diagram are used to show the final normalized wavelength, λ/h, which evolved from the initial values, λ_o/h_o, represented by crosses.

The initially plane interface started to become visibly irregular at ~4% BS in all models with $5 < \lambda/h \leq 40$ (Fig. 5a). Although inflections are obvious in the initially plane interface in the range $2 \leq \lambda/h \leq 4$ (Figs. 5c & d), it was found impossible to decide which of the two geom-

Table 1. Initial conditions in the experiments

Exp. series	Exp. No.	Wavelength initial λ_o (cm)	Thickness initial h_o (cm)	Normalized wavelength λ_o/h_o	Amplitude initial a_o (cm)	Viscosity ratio initial $m = \eta_L/\eta_H$*	a_o/h_o	$a_o/h_o \times 100$
S	S-1	2.5	0.2	12.50	0.025	1/2.2	0.125	12.50
	S-2	2.5	0.1	25.00	0.025	1/2.2	0.250	25.00
	S-3	2.5	0.3	8.30	0.025	1/2.2	0.083	8.33
	S-4	2.5	0.4	6.25	0.025	1/2.2	0.063	6.30
	S-5	2.5	0.6	4.20	0.025	1/2.2	0.042	4.20
	S-6	2.5	1.25	2.00	0.025	1/2.2	0.020	2.00
	S-7	2.5		one interface†				
C	C-1	3.1	0.1	31.00	0.025	1/2.2	0.250	25.00
	C-2	3.1	0.2	15.50	0.025	1/2.2	0.125	12.50
L	L-1	4.0	0.1	40.00	0.025	1/2.2	0.250	25.00
	L-2	4.0	0.2	20.00	0.025	1/2.2	0.125	12.50

*η_L = effective viscosity of layer, η_H = effective viscosity of host.
†a_o = 0.04–0.046.

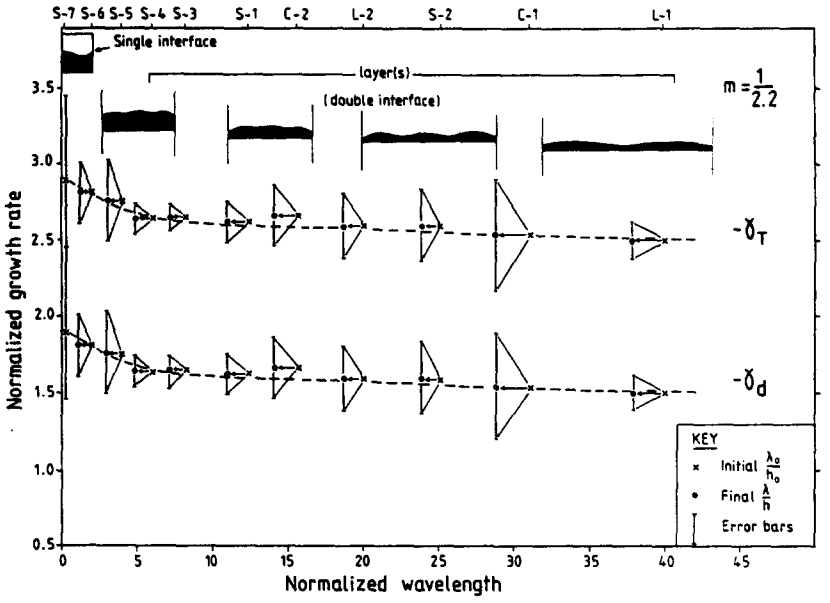

Fig. 4. Total normalized growth rate, γ_T, and dynamic growth rate, γ_d, for asymmetric mullions and a single interface plotted against normalized wavelength. The curve of γ_T indicates that for a viscosity contrast $m = 1/2.2$ asymmetric experimental mullions show no tendency to develop a dominant wavelength. Crosses represent the initial λ_o/h_o, while dots represent λ/h at ~15% BS for each model. The γ_d is negative and 1.0 must be subtracted to obtain γ_T; the negative sign indicates compression along the layer. Notice the increase in growth rate towards the single interface.

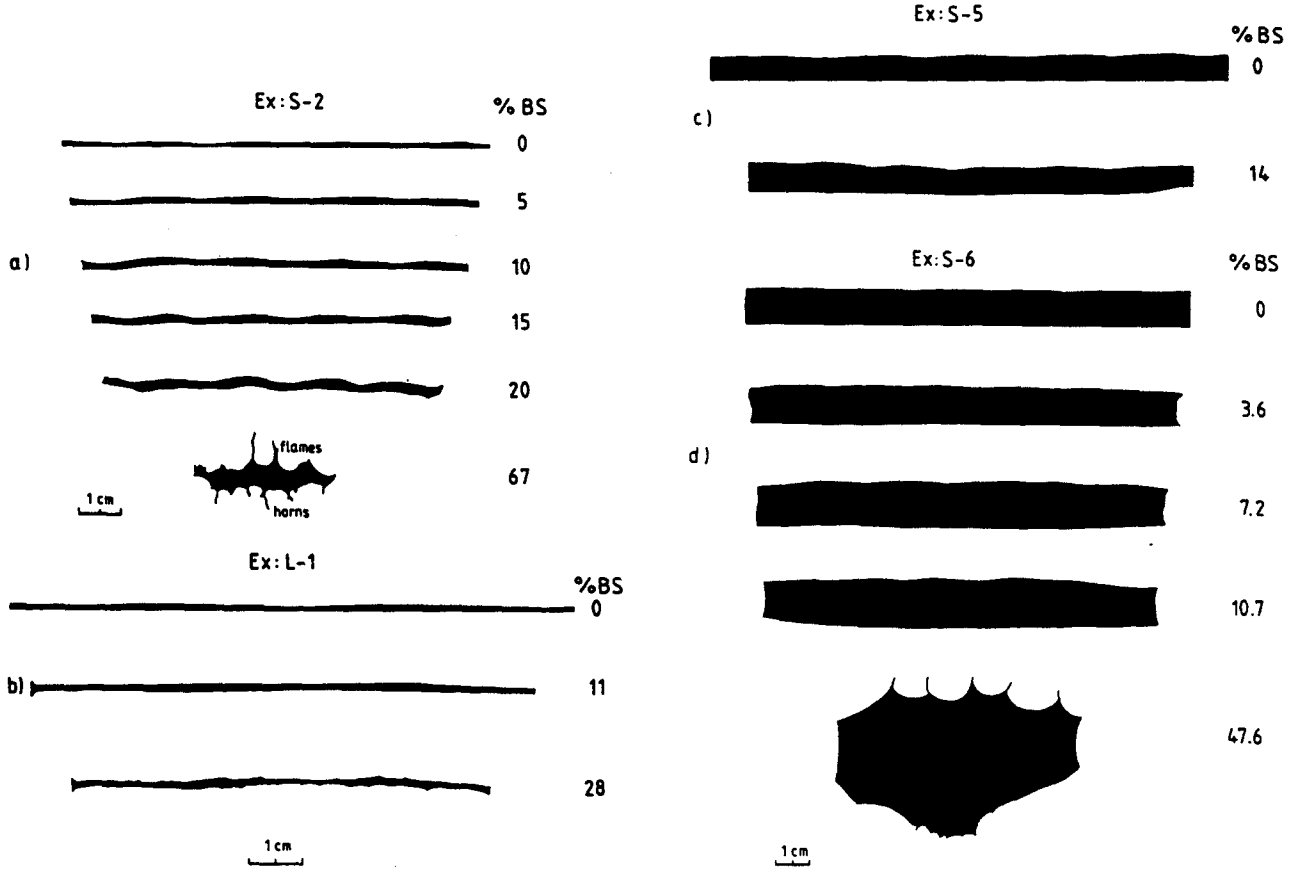

Fig. 5. Experimental mullions at different amounts of bulk shortening (% BS), starting with an asymmetric geometry. In all experiments Material B (see Fig. 2) represents the incompetent layer, while the competent host was represented by Material A (see Fig. 2). (a) Experiment S-2: the geometric forms of the incompetent layer interfaces become antisymmetric and fold-like at ~20% BS; (b) experiment L-1: illustration of an initially long wave breaking up into a number of small waves (range $25 < \lambda/h < 40$); (c) experiment S-5: unclear geometric relationship between the two interfaces of the incompetent layer (range $2 \leq \lambda/h < 5$); (d) experiment S-6: this shows no clear tendency towards a dynamic interaction between the participating incompetent layer interfaces, even at 47.6% BS (range $1 \leq \lambda/h \leq 2$), probably because the layer became too thick relative to the initial wavelength.

etries was preferred; pinch-and-swell or fold-like mullions. There seems to be some tendency for a pinch-and-swell-like geometry to precede a fold-like geometry in some experiments with long initial wavelengths (e.g. at 11% BS, Fig. 5b). For the experimental conditions described in this paper, particularly at such a low viscosity contrast, long initial waves, i.e. $\lambda/h > 25$, are not favoured and they break into smaller waves with quite clear fold-like geometries at about 28% BS (Fig. 5b). Although the purpose of this experimental work was not to investigate the changes in geometry at high bulk shortening, a few models were deformed to ~70% BS (Figs. 5a & d) to illustrate that these experimental mullions developed in the same general pattern as described by Sokoutis (1987). The difference is that mullions are obvious at ~30% BS at a low viscosity ratio (m = 1/2) while they appear earlier, at ~25% BS, for higher viscosity ratios ($m \simeq 1/190$ or $m \simeq 1/321$—in Sokoutis 1987).

Growth rates

Growth rate is the most useful parameter for investigating the tendency of experimental mullions to develop a dominant wavelength. The total growth, γ_T, at any stage was measured for every experiment as described in Sokoutis (1987). The dynamic growth, γ_d (the growth due to the secondary flow responsible for generating the deformation structures), is calculated by simply subtracting the kinematic growth, γ_K (the growth due to the primary flow responsible for uniform thickening and shortening) from the total growth (Fig. 4).

Figures 6(a)–(c) demonstrate that even for the low viscosity contrast of m = 1/2, mullions grow at a uniform rate up to 15% BS but then cease to grow at a certain amplitude (Fig. 6b). They then decrease in amplitude as the incompetent material is squeezed out of the closing cusps back into the incompetent layer which continues to shorten by uniform thickening alone.

Growth rates in a single interface

In experiments in which two interfaces bound a single layer, by the time the thickness of the layer exceeds the equivalent of one wavelength, the strain perturbations of the two interfaces cease to affect each other and we are effectively dealing with two single interfaces in the same model. However, these two contacts now have finite structures and are therefore inappropriate for studying the early growth rates of structures in a single interface. To do this, a model was constructed with a single interface and the amplification rates of the two initial central cusps were monitored.

According to infinitesimal theory there should be no dynamic growth (γ_d = 0), only kinematic growth (γ_K = 1) in a shortened single interface. However, as Fig. 4 shows, experimental findings are in total disagreement with this prediction (Fig. 7).

In the range $5 < \lambda/h < 25$ the dynamic growth shows no particular maximum, implying no preference for any

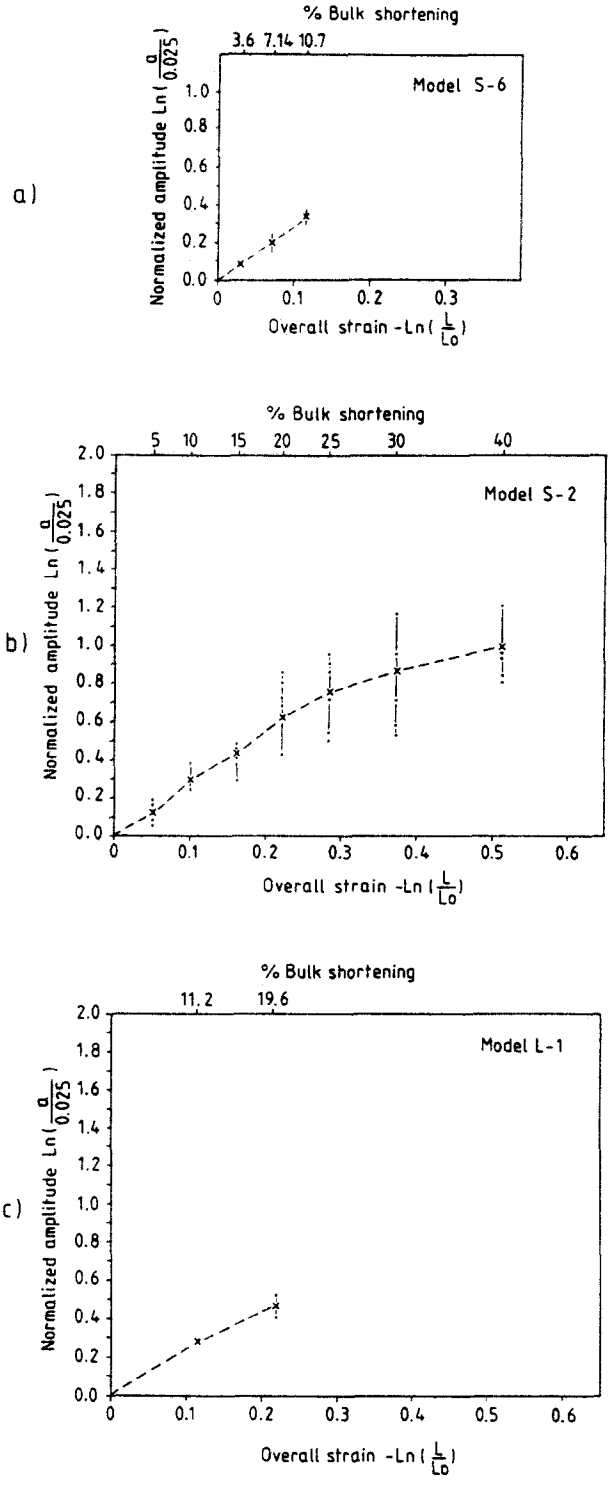

Fig. 6. (a–c) Normalized amplitude of cusps plotted against overall strain. Dots represent data points, crosses the arithmetic mean. The examples are from models S-6, S-2 and L-1, respectively (starting m = 1/2.2). For model S-2 the growth rate (γ_T) was plotted up to ~40% BS, simply to illustrate the change in growth mechanism (after ~25% BS). The slope of the linear part of the curve (~15% BS) was used for the growth rate calculation in Fig. 4.

wavelength (Fig. 4). By increasing the range in initial normalized wavelength to $25 < \lambda/h < 40$, the curve changes character and the dynamic growth starts to drop (Fig. 4). This smooth drop means that initially long waves are not preferred and break down into a number

of smaller waves above ~28% BS (Fig. 5b). This may be due to very small irregularities which exist at the onset of the experiment and grow faster in amplitude than the initial long wave.

DISCUSSION

Single interface and dominant wavelength (λ_d)

One of the most interesting questions raised by these experiments is why the perturbation in the single interface has a higher dynamic growth than those which are supposed to involve co-operation of two interfaces.

Theoreticians have predicted no dynamic instability at a single quasi-planar interface, whether the homogeneous materials are Newtonian (Biot 1965, Smith 1975, Fletcher 1982) or not (Fletcher 1974, 1982, Smith 1979). However, all these theories are for infinitesimal strains, and experiments are necessary in order to explore finite strain effects. Cobbold (1969a, figs. 3–6) found experimentally that initial irregularities in a single interface in Newtonian fluids amplified faster than kinematically and Fig. 7 demonstrates the same in non-Newtonian fluids. This effect may be due to the fact that the experiments were carried out under different boundary conditions than those treated by the theory. A possible deviation from the theoretical conditions derives from the lubricated sides of the model. If the boundaries are nearly frictionless they may act as mirror planes of symmetry, which means that in effect a multilayer system is modelled. The growth rates in such models are expected to differ from those of a single interface between two half spaces. This effect was not evaluated quantitatively.

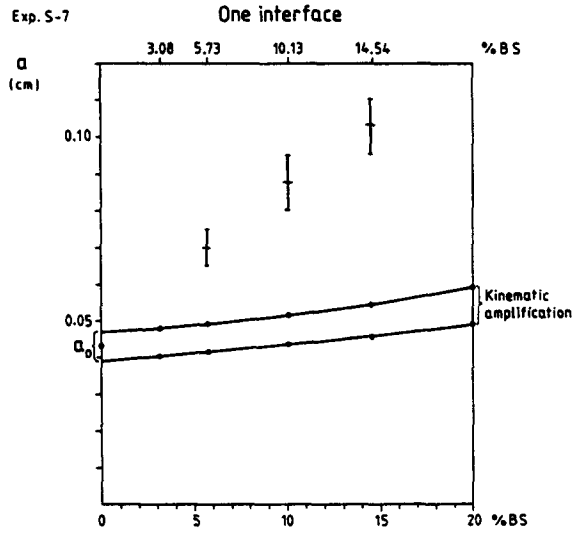

Fig. 7. The amplitude a of an induced waviness plotted vs % bulk shortening (BS) for the deformed single interface at different stages of deformation. The 'cusps' were chosen from the central part of the induced waviness of the interface with slight difference in initial amplitude, a_0. Notice that the total amplitude and its rate of amplification exceed those predicted by the infinitesimal theory, which indicates that only kinematic amplification should occur (where a_0 is the initial induced amplitude).

Theoretically no dominant wavelength is likely in a single interface. This is because there is no length scale fixed by two interfering interfaces.

Ramsay (1967, p. 383) reported a dominant wavelength in a shortened experimentally single interface but gave insufficient details about his experiment to be sure why. Ramsay's results may have misled Davies (1984, p. 428), who also proposed a dominant wavelength produced by shortening parallel to the contact between two rheologically different rocks. Initial wavelength(s) could amplify but this does not make them dominant.

Mullions in a single layer

The deformation of two near interfaces in a single layer is expected to lead to coupling in the sense that the secondary inhomogeneous flows at each interface co-operate. Smith (1977), however, did not predict how close the two interfaces should be for such co-operation to select the dominant wavelength. The initial conditions invoked by Smith differed from those used here.

Sokoutis (1987) studied the development of mullions in incompetent layers with two ostensibly planar and parallel interfaces. However, as in natural single layers, small initial irregularities can always be assumed in experiments, and there is no reason to expect much difference in their amplitudes in either interface.

In this work the initial perturbations were deliberately exaggerated on one interface so that the starting configuration was strongly asymmetric (Chadwick 1976) (Fig. 1c).

Dynamic interaction between the two interfaces causes the initially plane surface to become perturbed and allows the irregularities in the initially plane interface to catch up and reach amplitudes nearly equal to those of the other interface. Such interaction is expected so long as the two surfaces are closer than one wavelength. Experiments where shortening is more than ≈20% BS (e.g. Fig. 5a) tend to develop antisymmetric (fold-like) mullions. At ≈67% BS the geometrical shape changes even at $m = 1/2$ are similar to those at $m = 1/190$ (Sokoutis 1987) (see Figs. 5a & d at 67% and 47.6%, respectively). This may not be true if the host fails as a brittle solid. However, what may be mistaken as shears associated with mullions may be the tracks along which cusps have closed up to form flames and then withdrawn.

Structural growth rates

The direct effect of reducing the viscosity contrast between the incompetent layer and the competent host from a value of 1/190 (Sokoutis 1987) to the value of ~1/2 used here is that the mullions grow more slowly. Figure 6(b) shows that mullions amplify at a constant rate up to ~15% BS but then slow down and thereafter close and join to form flames, etc. (Sokoutis 1987). Similar decreases in dynamic growth rates occur in folds

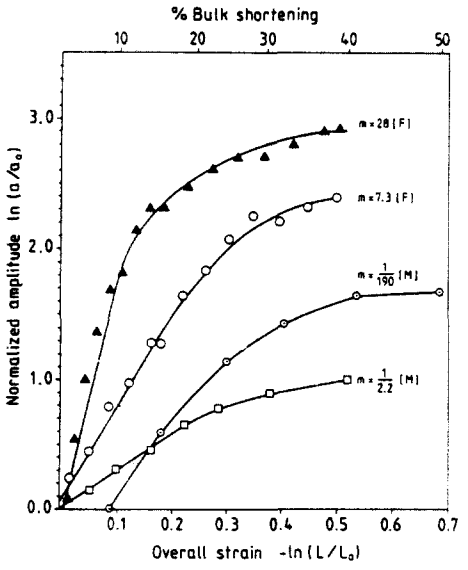

Fig. 8. Comparison between growth rates of folds (Neurath & Smith 1982) and mullions (Sokoutis 1987 and this work) from physical model experiments at nearly identical bulk-strain rates (10^{-4} s^{-1}). Notice that high viscosity contrast mullions have lower growth rates than low viscosity contrast folds (where m is the viscosity contrast. F is for folds and M is for mullions).

(Fig. 8) and boudins (Neurath & Smith 1982, fig. 6). This change in deformation mechanism is most probably due to a combination of different effects (i.e. of material properties and geometry), of which the most important seems to be the strain-rate softening effect (Neurath & Smith 1982, Sokoutis 1987). Strain-rate softening is especially important in experiments in which the viscosity contrast starts low and then decreases further during the deformation (because the experiment is not quite at constant strain rate). However, since the growth rate is computed from the slope of the linear part of the curve (i.e. BS $\leq$ 15%), such strain-rate softening can only have a minor influence on the results (Figs. 6a–c). The strain-rate softening effect would be increased if the amplitude of the initial perturbations in the interface were higher. This effect was minimized in all experiments by keeping the initial perturbation amplitudes at 0.025 cm. However, this also meant that measuring accuracy was sacrificed. As in Sokoutis (1987), the growth rates of experimental mullions were higher than those predicted from the infinitesimal non-Newtonian theory of Smith (1977). This theory also underestimated the much faster growth rates of boudinage in wax-model experiments (Neurath & Smith 1982).

Asymmetric mullions and λ_d

Because there were no preferred growth rates at any normalized wavelengths, the results (Fig. 4) illustrate the complete lack of a dominant wavelength under the experimental conditions. This may have been because one of the interfaces bounding the layer was initially planar. Although the initially perturbed interface grew dynamically, the planar interface does not appear to have co-operated in that growth, at least during the first stages of deformation (i.e. ~10% BS). Indeed the planar interface may have hindered the growth of the initially sinusoidal interface by acting as a 'competent wall' missing in the one interface situation. Any such hindrance is stronger for $\sim\lambda/h > 5$ and weaker for $\sim\lambda/h < 5$ (see Fig. 4), and could account for the slight decrease of the growth rate towards long wavelengths.

Co-operation between the two interfaces, because of their similarity, could still pose a problem for a dominant wavelength to be clearly developed for a viscosity contrast as low as 1/2. The dominant wavelength is not expected to be clear even in buckling of competent single layers with viscosity contrasts below 10 (Ramberg 1979). It is even less likely for mullions, which amplify more slowly than folds. The instability is very non-selective of wavelength.

The single interface model (model S-7, Fig. 5) shows slightly faster growth than the rest. However, this does not necessarily indicate a dominant wavelength.

Symmetric mullions?

The only possible symmetric inflections in the initially planar interface occurred at BS < 11% in layers with long wavelengths (i.e. $\lambda/h > 20$). These low amplitude, long wavelength pinch-and-swell-like structures agree with the predictions of infinitesimal theory, but even these became antisymmetric at BS > 11%. A possible explanation is that the mechanism for developing lobe and cusps is a finite amplitude mechanism qualitatively different from the infinitesimal amplitude mechanism responsible for symmetric structures with pinch-and-swell geometry. If this is so, the finite lobe and cusp generating mechanism swaps the initial symmetric inflections to generate antisymmetric inflections at BS > 11%.

CONCLUSIONS

(1) Mullions in a single interface amplify actively rather than kinematically in non-Newtonian fluids, and this becomes obvious at lower finite shortenings than in the Newtonian fluids reported by Cobbold (1969a).

(2) The absence of a length scale in a single interface suggests that a dominant wavelength is unlikely, despite Ramsay (1967) and Davies (1984) proposing a dominant wavelength without explaining how.

(3) The experiments reported here demonstrate that mullions initiated asymmetrically in layers with a viscosity contrast of $\simeq$1/2 show no tendency to develop a dominant wavelength.

(4) The measured growth rates of experimental asymmetric mullions are lower than those studied previously (Sokoutis 1987). The viscosity contrast was lower ($m \simeq$ 1/2) and the initial asymmetry may have hindered dynamic interaction. As Smith (1977) studied neither asymmetric mullions nor finite deformations, the growth rates reported here cannot be compared directly with his theoretical predictions.

(5) Even for $m \simeq$ 1/2 mullions close up to become

flames and combine to become horns (see Fig. 5a, 67% BS) as already demonstrated for higher viscosity contrast (Sokoutis 1987).

(6) Despite some ambiguity at low strains (≤11% BS), incompetent layers exhibit a preference towards antisymmetric (fold) mullions in both nature and experiment at finite strains (Sokoutis 1987 and this work).

(7) An additional genetic term(s) is needed to distinguish mullions due to shortening from structures of similar geometries produced by other mechanisms. Conclusion (6) above suggests that Wilson's (1953) term 'fold mullions' is most appropriate for both shortened single interfaces and single layers.

Acknowledgements—I am greatful to Professors C. J. Talbot and H. Ramberg for their interest, encouragement and guidance throughout this work. Drs H. Schmeling and R. Weijermars are sincerely thanked for fruitful discussions. Dr P. Cobbold and an anonymous reviewer are thanked for their thoughtful and very helpful comments. Miss. K. Gløersen is thanked for typing the manuscript and Mrs Ch. Wernström for drafting the figures.

REFERENCES

Bates, R. L. & Jackson, J. A. 1980. *Glossary of Geology*. American Geological Institute, Virginia.

Biot, M. E. 1965. Theory of viscous buckling and gravity instability of multilayers with large deformation. *Bull geol. Soc. Am.* **76**, 371–378.

Chadwick, P. 1976. Tectonic structures—a classification. *Tectonophysics* **30**, T3—T9.

Cobbold, P. R. 1969a. An experimental study of the formation of lobe and cusp structures by shortening of an initial sinusoidal contact between two materials of different viscosity. Unpublished B.Sc. thesis, University of London.

Cobbold, P. R. 1969b. Structural geology of the Val Camadra–Greina area, Ticino, Switzerland. Unpublished B.Sc. thesis, University of London.

Cobbold, P. R. 1976. Unified theory of the onset of folding, boudinage, and mullion structures: Discussion. *Bull. geol. Soc. Am.* **87**, 1663.

Davies, G. H. 1984. *Structural Geology of Rocks and Regions*. John Wiley & Sons, New York.

Dieterich, J. H. & Onat, E. T. 1969. Slow finite deformations of viscous solids. *J. geophys. Res.* **74**, 2081–2088.

Fletcher, R. C. 1974. Wavelength selection in the folding of a single layer with power law rheology. *Am. J. Sci.* **274**, 1029–1043.

Fletcher, R. C. 1982. Analysis of the flow in layered fluids at small, but finite, amplitude with application to mullion structures. *Tectonophysics* **81**, 51–66.

McClay, K. R. 1976. The rheology of plasticine. *Tectonophysics* **33**, T7–T15.

Neurath, G. & Smith, R. B. 1982. The effect of material properties on growth rates of folding and boudinage: experiments with wax models. *J. Struct. Geol.* **4**, 215–229.

Onogi, S. & Matsumoto, T. 1981. Rheological properties of polymer solutions and melts containing suspended particles. *Polymer Engng Rev.* **1**, 45–87.

Pfiffner, O. A. & Ramsay, J. G. 1982. Constraints on geological strain rates: arguments from finite strain states of naturally deformed rocks. *J. geophys. Res.* **87**, 311–321.

Ramberg, H. 1970. Folding of laterally compressed multilayers in the field of gravity. II. Numerical examples. *Phys. Earth & Planet. Interiors* **4**, 83–120.

Ramberg, H. 1979. Folding of a single viscous layer: exact infinitesimal amplitude solution—discussion. *Tectonophysics* **56**, 321–326.

Ramberg, H. 1981. *Gravity, Deformation and the Earth's Crust* (2nd edn). Academic Press, London.

Ramsay, J. G. 1967. *Folding and Fracturing of Rocks*. McGraw-Hill, New York.

Smith, R. B. 1975. Unified theory of the onset of folding, boudinage, and mullion structure. *Bull. geol. Soc. Am.* **86**, 1601–1609.

Smith, R. B. 1977. Formation of folds, boudinage, and mullions in non-Newtonian materials. *Bull. geol. Soc. Am.* **88**, 312–320.

Smith, R. B. 1979. The folding of a strongly non-Newtonian layer. *Am. J. Sci.* **279**, 272–287.

Sokoutis, D. 1987. Finite strain effects in experimental mullions. *J. Struct. Geol.* **9**, 233–242.

Talbot, C. J. 1983. Microdiorite sheet intrusions as incompetent time- and strain-markers in the Moine assemblage NW of the Great Glen fault, Scotland. *Trans. R. Soc. Edinb., Earth Sci.* **74**, 137–152.

Weijermars, R. 1986. Flow behaviour and physical chemistry of Bouncing Putties and related polymers in view of tectonic laboratory applications. *Tectonophysics* **124**, 325–358.

Weijermars, R. & Schmeling, H. 1986. Scaling of Newtonian and non-Newtonian fluid dynamics without inertia for quantitative modelling of rock flow due to gravity (including the concept of rheological similarity). *Phys. Earth & Planet. Interiors* **43**, 316–330.

Wilson, G. 1953. Mullion and rodding structures in the Moine Series of Scotland. *Proc. Geol. Ass.* **64**, 118–151.

Wilson, G. 1961. The tectonic significance of small-scale structures, and their importance to the geologist in the field. *Annls. Soc. géol. Belg.* **84**, 510–517.